Far Infrared Reflection Spectra and Lattice Vibrations of $CsNiCl_3$ Crystal

Kenji AKIYAMA, Yoshiyuki MORIOKA, and Ichiro NAKAGAWA

Department of Chemistry, Faculty of Science, Tohoku University, Aoba, Aramaki, Sendai 980

(Received July 7, 1977)

The frequencies of the transverse (TO) and longitudinal (LO) modes of the infrared active vibrations of the crystal $CsNiCl_3$ were obtained from the polarized far infrared reflection spectra. The polarized Raman spectra were also measured. The calculation of the TO and LO frequencies near the center of the Brillouin zone was made on the basis of a rigid ion model which includes effective ionic charges and interionic repulsive force constants. A set of potential constants and effective ionic charges were determined from the observed values of the TO and LO frequencies and Raman frequencies using the least-squares method. The short-range force constant associated with the nickel ion to the chlorine ion indicates that some amount of covalent character is included in this bond.

Cesium nickel trichloride, $CsNiCl_3$, is a so-called ionic crystal which has a hexagonal perovskite-like structure. A large number of double salts of the AMX_3 type (where A is a large univalent cation, M a divalent metal ion and X a halogen ion) are isomorphous to $CsNiCl_3$. The infrared spectra of these crystals reported, however, have been restricted to the transmission spectra of powder samples.[1] McPherson and Chang reported the infrared transmission spectra of powder sample of $CsNiCl_3$.[1] Adams and Smardzewski studied the polarized far infrared transmission spectra of a thin film of $(CH_3)_4NMnCl_3$,[2] the structure of which is closely related to that of $CsNiCl_3$.

Each of the transverse(TO) and the longitudinal (LO) frequencies of the infrared active modes can be determined by the infrared reflection spectra. In the present study we have measured the polarized far infrared reflection spectra and polarized Raman spectra of $CsNiCl_3$. Using the observed frequencies of the normal modes, the short-range potential constants and the effective ionic charges were obtained by means of the normal coordinate analysis for the optically active lattice vibrations.

The crystal structure of $CsNiCl_3$ as shown in Fig. 1 belongs to hexagonal system with the space group D_{6h}^4 ($P6_3/mmc$).[3] Bravais unit cell consists of two formula units of $CsNiCl_3$. In this hexagonal structure, the nickel ions are located in the center of octahedra formed by chlorine ions and the chains of slightly compressed $NiCl_3$ octahedra sharing opposite faces run along the c axis of the crystal. The cesium ions are on the planes formed by three chlorine ions. The result of the factor group analysis on the basis of this structure is summarized in Table 1.

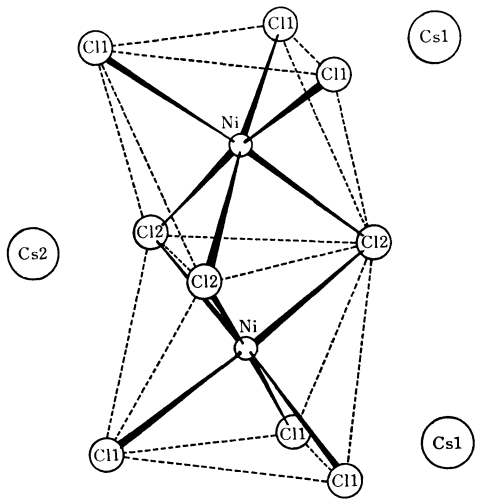

Fig. 1. Crystal structure of $CsNiCl_3$.

TABLE 1. FACTOR GROUP ANALYSIS FOR $CsNiCl_3$

D_{6h}	N[a]	T[b]	$N-T$[c]	Activity
A_{1g}	1	0	1	(xx+yy, zz)
A_{2g}	1	0	1	
B_{1g}	2	0	2	
B_{2g}	0	0	0	
E_{1g}	1	0	1	(yz, zx)
E_{2g}	3	0	3	(xx−yy, xy)
A_{1u}	0	0	0	
A_{2u}	3	1	2	z
B_{1u}	1	0	1	
B_{2u}	2	0	2	
E_{1u}	4	1	3	x, y
E_{2u}	2	0	2	

a) Total freedom. b) Acoustic modes. c) Optical active modes.

Experimental

Sample Preparation. The powder sample of $CsNiCl_3$ was crystallized by evaporation from the hot concentrated aqueous solution of CsCl and $NiCl_2$ in a 1 : 1 mole ratio, and was heated in vacuum for several hours. Completely dehydrated salt was molten in vacuum, filtered through quartz wool and sealed into quartz ampoule. The single crystal was grown from the molten salt by the Bridgman method. Crystal cleaves readily along the (110) plane and this cleavage plane was used for reflection measurement without polishing. For the Raman measurement, the single crystal was polished to a cube, three planes of which were parallel to (100), (001) and (010) planes, respectively.

Spectral Measurement. Polarized far infrared reflection spectra were recorded using a Hitachi 070 far infrared interferometer equipped with a wire-grid polarizer. The reflectivities for the lights polarized perpendicular and parallel to the c axis were measured. The incident angle was fixed at about 20°. The infrared transmission spectrum of the Nujol mull of powder sample was also measured. The polarized Raman spectra of the single crystal were measured by a Narumi double monochromator with a 632.8 nm line

of a He–Ne laser as a source.

Results

Figures 2a and 3a show the observed reflectivities for the lights polarized perpendicular and parallel to the c axis, respectively. The refractive index n, the absorption index k, and the real and imaginary parts of the dielectric constant, ε' and ε'', were obtained from the observed reflectivities using the Kramers-Kronig relation assuming the normal incidence.[4] The obtained results are shown in Figs. 2 and 3 together with the observed reflectivities. The TO frequencies are given by the maxima of the imaginary part of the dielectric constant and the corresponding LO frequencies are given by the frequencies where the real part of the dielectric constant becomes zero in changing from negative to positive values.[5] However, in the frequency region 270—100 cm^{-1} of Fig. 2c the real part of the dielectric constant does not become zero, and the OL frequency 180 cm^{-1} for ν_9(LO) was obtained by the frequency where Im$(-1/\varepsilon)$ has maximum value.[6]

It is clear that the TO and LO frequencies obtained from the reflectivities for the lights polarized perpendicular and parallel to the c axis correspond to the E_{1u} and A_{2u} modes of the factor group D_{6h}, respectively. The all infrared active vibrational modes predicted from the factor group analysis shown in Table 1 have been observed. The assignment of the five observed TO frequencies to the symmetry species is consistent with that of $(CH_3)_4$ $NMnCl_3$ by Adams and Smardzewski, although the structures of $CsNiCl_3$ and $(CH_3)_4N$-

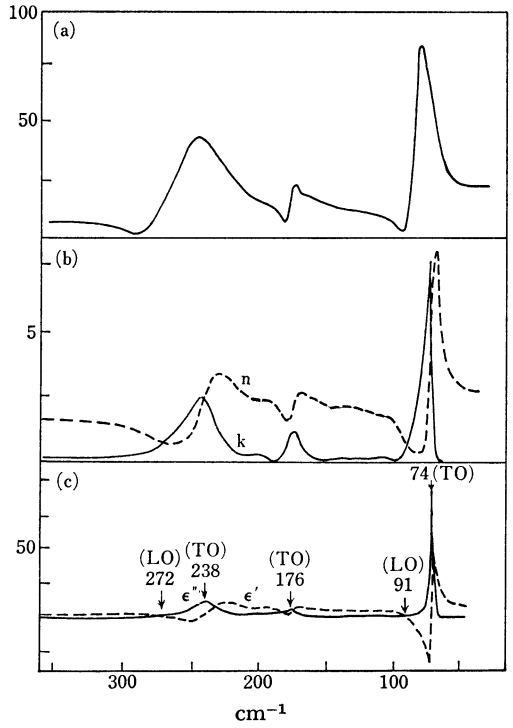

Fig. 2. (a) Percent reflectivity, (b) refractive index n, and absorption index k, and (c) real and imaginary parts of the dielectric constant, ε' and ε'', of $CsNiCl_3$ for the light polarized perpendicular to the c axis.

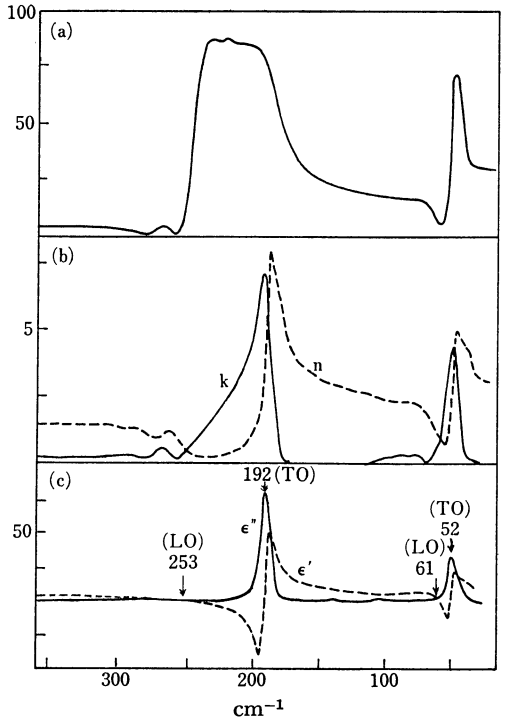

Fig. 3. (a) Percent reflectivity, (b) refractive index n and absorption index k, and (c) real and imaginary parts of the dielectric constant, ε' and ε'', of $CsNiCl_3$ for the light polarized parallel to the c axis.

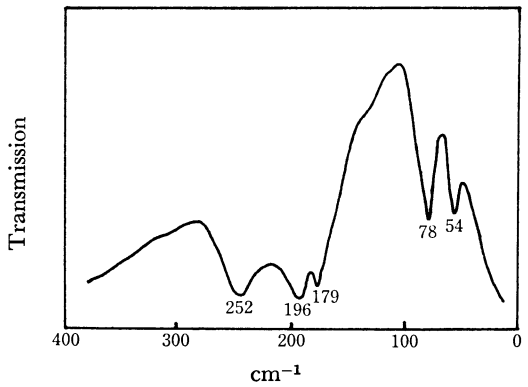

Fig. 4. Transmission spectrum of the powder sample of $CsNiCl_3$.

$MnCl_3$ are not exactly the same.

A short comment should be made on the transmission spectrum of the powder sample. Our result of the powder sample shown in Fig. 4 is in agreement with the spectrum by McPherson and Chang. The maximum absorption frequencies are slightly higher than the TO frequencies determined from the reflection spectra, which may be attributable to the crystal size effect.[7]

Figure 5 shows the observed Raman spectra in which the notations by Damen *et al.*[8] are indicated. On the basis of the Raman tensors of D_{6h} symmetry shown in Table 1 the bands at 264 and 140 cm^{-1} are assigned to the A_{1g} and E_{1g} modes, respectivery, and the bands at 190 and 52 cm^{-1} are assigned to the E_{2g} modes. Observed frequencies and vibrational

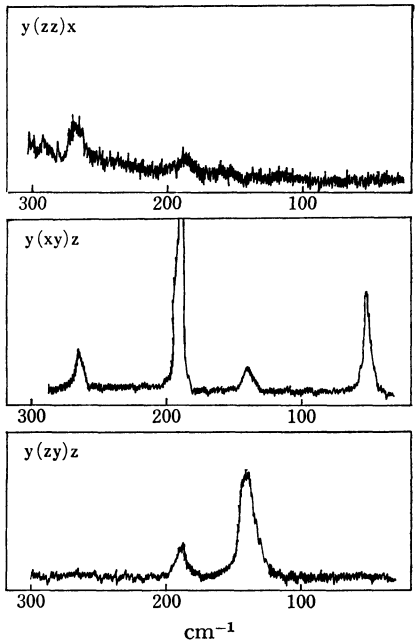

Fig. 5. Polarized Raman spectra of $CsNiCl_3$. Experimental z axis is coincident with the c axis of the crystal.

Table 2. Observed and calculated frequencies of infrared and raman active vibrations in $CsNiCl_3$

		Obsd (cm^{-1})	Calcd	
			Case I (cm^{-1})	Case II (cm^{-1})
A_{1g}	ν_1	264	241	247
E_{1g}	ν_2	140	167	164
E_{2g}	ν_3	190	199	204
	ν_4		166	163
	ν_5	52	64	64
A_{2u}	ν_6(TO)	192	199	199
	ν_7(TO)	52	47	48
	ν_6(LO)	253	257	257
	ν_7(LO)	61	63	63
E_{1u}	ν_8(TO)	238	227	225
	ν_9(TO)	176	164	167
	ν_{10}(TO)	74	75	72
	ν_8(LO)	272	268	267
	ν_9(LO)	180	182	184
	ν_{10}(LO)	91	86	84

assignments are summarized in Table 2.

Normal Coordinate Analysis

Optically active vibrational frequencies are calculated according to the method of Shimanouchi, Tsuboi and Miyazawa.[9] Equations of motion for a rigid ion model are written in terms of the Cartesian displacement coordinates of component ions of a whole crystal;

$$4\pi^2\nu^2\boldsymbol{MX} = (\boldsymbol{F}_X^R + \boldsymbol{F}_X^C)\boldsymbol{X}, \tag{1}$$

$$\boldsymbol{F}_X^C = \boldsymbol{ZCZ}, \tag{2}$$

where $\boldsymbol{X}$ is column matrix corresponding to the Cartesian displacement coordinates and $\boldsymbol{M}$ and $\boldsymbol{Z}$ are the diagonal matrices specifying the masses and ionic charges. $\boldsymbol{F}_X^R$ and $\boldsymbol{F}_X^C$ (or $\boldsymbol{C}$) denote the short-range repulsive potential and the long-range Coulomb potential, respectively. The secular equation

$$|\boldsymbol{M}^{-1}(\boldsymbol{F}_X^R + \boldsymbol{F}_X^C) - \boldsymbol{E}\lambda| = 0 \quad (\lambda = 4\pi^2\nu^2), \tag{3}$$

is set up and the TO and LO frequencies of crystal are calculated.

Since the TO-LO splittings for the infrared active modes arise from the macroscopic electric field, the effective ionic charges are estimated by using the TO-LO splitting. The relation between the effective ionic charges and the TO-LO splittings is derived as[10]

$$8\pi\left(\frac{e_{Ni}^2}{m_{Ni}} + \frac{e_{Cs}^2}{m_{Cs}} + \frac{3e_{Cl}^2}{m_{Cl}}\right)\Big/ v_a = \sum_i \lambda_i^2(\mathrm{LO}) - \sum_i \lambda_i^2(\mathrm{TO}), \tag{4}$$

where m_{Ni}, m_{Cs}, and m_{Cl} are atomic masses, e_{Ni}, e_{Cs}, and e_{Cl} are effective ionic charges, v_a is the volume of the Bravais unit cell and λ_i is the frequency parameter ($\lambda_i = 4\pi^2\nu_i^2$) of the i-th vibration. For a condition of the electrical neutrality of a crystal as a whole, the effective ionic charges must satisfy the relation

$$Z_{Cs} + Z_{Ni} + 3Z_{Cl} = 0, \tag{5}$$

where $Z_i e = e_i$ (i=Ni, Cs, and Cl). From Eqs. 4 and 5, the relation among Z_{Ni}, Z_{Cs}, and Z_{Cl} is determined and therefore only one Z_i of the three becomes independent.

The long-range Coulomb part $\boldsymbol{F}_X^C$ is calculated from the effective ionic charges and the $\boldsymbol{C}$ matrix, which is obtained using Ewald's transformation according to the method derived by Kellerman.[11]

As for the short-range part $\boldsymbol{F}_X^R$, two different model force fields have been applied.

Case I; The central force type potential was assumed for all the interionic interactions.

Case II; The valence force type potential for the $NiCl_6$ structure and the central force type potential for the ion pairs, for which the nonbonded repulsions or the ionic interactions are expected to be appreciable, were assumed.

In case I, the potential energy of the crystal is given as

$$V = \frac{1}{2}\sum_{lk}\sum_{l'k'}{}' \varphi_{kk'}(r(lk:l'k')), \tag{6}$$

where $\varphi_{kk'}$ is the interaction potential between the k-th and k'-th ions and $r(lk:l'k')$ is the instantaneous distance between the k-th ion in the l-th unit cell and the k'-th ion in the l'-th unit cell. The short-range potential $\varphi_{kk'}$ is a function of only the distance between the two ions. The matrix elements of the short range part $\boldsymbol{F}_X^R$ are given as;

$$F_X^R(k\alpha,k'\beta) = -\sum_{l'}\left\{\frac{x_\alpha x_\beta}{r^2}\left[\varphi''_{kk'}(r) - \frac{1}{r}\varphi'_{kk'}(r)\right] + \frac{\delta_{\alpha\beta}}{r}\varphi'_{kk'}(r)\right\}\Big|_{r=r_0(lk:l'k')}$$

$$F_X^R(k\alpha,k\beta) = \sum_{k'(\neq k)}{}' F_X^R(k\alpha,k'\beta), \tag{7}$$

where $r_0(lk:l'k')$ denotes $r(lk:l'k')$ in the equilibrium arrangement and x_α is the α-Cartesian component

(α=x, y, and z) of $r_0(lk:l'k')$.

The ion pairs within a distance of 4.0 Å were taken into account, since the short-range repulsive force may become significant in this interionic distance. The following ten potential constants were taken;

$$K_1 = [\varphi''(\text{Ni-Cl})(r)]_{r=r_0(\text{Ni-Cl})},$$

$$k_1 = \left[\frac{1}{r}\varphi'(\text{Ni-Cl})(r)\right]_{r=r_0(\text{Ni-Cl})},$$

$$K_2 = [\varphi''(\text{Cs-Cl})_{\text{I}}(r)]_{r=r_0(\text{Cs-Cl})_{\text{I}}},$$

$$k_2 = \left[\frac{1}{r}\varphi'(\text{Cs-Cl})_{\text{I}}(r)\right]_{r=r_0(\text{Cs-Cl})_{\text{I}}},$$

$$K_3 = [\varphi''(\text{Cs-Cl})_{\text{II}}(r)]_{r=r_0(\text{Cs-Cl})_{\text{II}}},$$

$$k_3 = \left[\frac{1}{r}\varphi'(\text{Cs-Cl})_{\text{II}}(r)\right]_{r=r_0(\text{Cs-Cl})_{\text{II}}},$$

$$K_4 = [\varphi''(\text{Cl-Cl})_{\text{I}}(r)]_{r=r_0(\text{Cl-Cl})_{\text{I}}},$$

$$k_4 = \left[\frac{1}{r}\varphi'(\text{Cl-Cl})_{\text{I}}(r)\right]_{r=r_0(\text{Cl-Cl})_{\text{I}}},$$

$$K_5 = [\varphi''(\text{Cl-Cl})_{\text{II}}(r)]_{r=r_0(\text{Cl-Cl})_{\text{II}}},$$

$$k_5 = \left[\frac{1}{r}\varphi'(\text{Cl-Cl})_{\text{II}}(r)\right]_{r=r_0(\text{Cl-Cl})_{\text{II}}},$$

where subscripts I and II denote the inter-layer and intralayer ion pairs, respectively. (According to the numbering of the atoms in Fig. 1, the inter-layer ion-pairs include those of Cs_1–Cl_1, Cs_2–Cl_2, Cl_1–Cl_1, and Cl_2–Cl_2, and the intralayer ion pairs include those of Cs_1–Cl_2, Cs_2–Cl_1, and Cl_1–Cl_2). The interionic distances in the equilibrium arrangement are listed in Table 3.

There are 11 parameters to be determined; ten are the short-range repulsive force constants and one is the effective ionic charge. In the actual procedure, K_4, K_5, k_4, and k_5 were estimated from the nonbonded chlorine-chlorine interaction potential of Lennard-Jones 6—12 type,[12] and k_2 and k_3 were fixed —0.01 mdyn/Å and —0.006 mdyn/Å, respectively, which correspond to the values for —0.1 K_2 and —0.1 K_3*.

Table 3. Determined short-range force constants and effective ionic charges

Short range force constants				Corresponding interionic distances (Å)
Case I (mdyn/Å)		Case II (mdyn/Å)		
K_1	0.764 (±0.043)	K_1	0.739 (±0.048)	2.44
K_2	0.096 (±0.022)	K_2	0.085 (±0.020)	3.57
K_3	0.064 (±0.011)	K_3	0.059 (±0.010)	3.70
K_4	0.062	K_4	0.062	3.34
K_5	0.020	K_5	0.020	3.55
k_1	0.082 (±0.061)	H_1	0.015 (±0.013)	
k_2	−0.010	H_2	0.036 (±0.024)	
k_3	−0.006			
k_4	−0.003			
k_5	−0.000			
Effective ionic charges				
Z_{Cl} = −0.660				
Z_{Ni} = 1.462				
Z_{Cs} = 0.518				

Throughout this paper 1Å=0.1 nm, 1 mdyn/Å=10^2N/m.
The values in parentheses denote standard deviations.

The long-range Coulomb part was calculated from various sets of Z_i's and in each case the short-range repulsive force constants were determined by the least squares method using the observed vibrational frequencies. It was found that among the various sets of Z_i's only those for Z_{Cl}=—0.6——0.7 are physically significant. For the value of Z_{Cl} larger than —0.6 the effective ionic charge of cesium ion becomes negative and for the value smaller than —0.7, no physically significant frequencies are obtained for the low-frequency vibrational modes.

The set of the effective ionic charges shown in Table 3 gives a most satisfactory result. (The sum of the square deviations of the calculated frequencies from the observed ones becomes minimum for this set of Z_i's when Z_{Cl} is varied from —0.6 to —0.7). The calculated frequencies and the obtained short-range repulsive force constants are shown in Tables 2 and 3 as case I, respectively.

In case II, the short-range potential function is given as:

$$V = \frac{1}{2}\sum K_1(\Delta r^i_{\text{Ni-Cl}})^2 + \frac{1}{2}\sum H_1(r^0_{\text{Ni-Cl}}\Delta\alpha^i(\text{Cl}_1\text{-Ni-Cl}_1))^2 + \frac{1}{2}\sum H_2(r^0_{\text{Ni-Cl}}\Delta\alpha^i(\text{Cl}_1\text{-Ni-Cl}_2))^2 + \frac{1}{2}\sum K_2(\Delta r^i_{(\text{Cs-Cl})_{\text{I}}})^2 + \frac{1}{2}\sum K_3(\Delta r^i_{(\text{Cs-Cl})_{\text{II}}})^2 + \frac{1}{2}\sum K_4(\Delta r^i_{(\text{Cl-Cl})_{\text{I}}})^2 + \frac{1}{2}\sum K_5(\Delta r^i_{(\text{Cl-Cl})_{\text{II}}})^2, \quad (8)$$

where K_1 is the Ni–Cl bond stretching force constant, K_2 and K_3 are those for the interaction between the cesium and chlorine ions, K_4 and K_5 are the repulsive force constants between two chlorine ions and H_1 and H_2 are the Cl_1–Ni–Cl_1 and Cl_1–Ni–Cl_2 bending force constants. The calculated frequencies and the force constants obtained by the least-squares method are shown in Tables 2 and 3 as case II, respectively.

In the procedure of the force constant calculation mentioned above, 4 force constants in case I and 5 force constants in case II were determined by the least-squares method using 14 observed frequencies. The standard deviations are given for these force constants in Table 3.

Discussion

The spectrum consisting of the five TO vibrations (two A_{2u} and three E_{1u} modes) as shown in Figs. 2, 3, and 4 reveals a typical feature characteristic of the two-layer type of the AMX_3 perovskite structure. The powder transmission spectrum of $CsNiF_3$ which has the same structure is similar to that of $CsNiCl_3$, although the lowest band was not observed for $CsNiF_3$ due to the limitation of the utilized spectrometer.[14]

The observed infrared and Raman frequencies are well explained by the model used in the calculation.

* The values of k_2 and k_3 do not affect the calculated frequencies significantly. Here, the same assumption as in the case of CdX_2 was made.[13]

This model is simple but it includes both the short-range potential and the long-range Coulomb potential in terms of effective ionic charges and explains quantitatively the splittings of the TO and LO frequencies.

In Table 2 the calculated frequencies by the converged set of force constants are not very different in both cases. The short-range potential of the type in case II has been often used for the complex salts such as K_2PtCl_6 and it has been found that this type of the potential is quite satisfactory to interpret the lattice vibrations due to the interaction between the complex ion and the outer ion as well as the intra-ligand vibrations. However, in the case of more ionic crystals like $CsNiCl_3$, the central force type potential may be more adequate for the analysis of the interionic vibrations. In this type of the potential the first derivatives of the interionic potential $\varphi'_{kk'}$ cannot be neglected. In $CsNiCl_3$, k_1, which corresponds to the first derivative of the interaction potential between the Ni and Cl ions, amounts to a significant value as shown in Table 3. A physically significant K_1 value (the second derivative of the Ni–Cl interaction potential) may be obtained, by taking k_1 into consideration. The neglect of the first derivatives in the central force potential cannot explain both Raman and infrared observed frequencies simultaneously, as in the case of CdX_2.[13]

The value of the Ni–Cl stretching force constant K_1 is obtained as 0.764 mdyn/Å in case I and 0.739 mdyn/Å in case II. These values are definitely smaller than the value 1.8 mdyn/Å of the Ni–C stretching force constant in $Ni(CO)_4$[15] but are comparable to the value 0.977 mdyn/Å for the Ni–F stretching force constant in $KNiF_3$,[16] indicating that some amount of covalent character is included in the Ni–Cl bond.

The ionic displacements for each vibration are shown in Fig. 6 on the basis of the eigenvectors $\boldsymbol{L}_x$ for the secular equation (3). The $\nu_5(E_{2g})$, $\nu_7(A_{2u})$, and ν_{10} (E_{1u}) are the translational lattice modes, and the others are the vibrations of the $NiCl_6$-octahedra. The Ni–Cl stretching and Cl–Ni–Cl bending vibrations are not clearly distinguished unlike those for the cubic perovskite fluorides. However, the $\nu_6(A_{2u})$ and $\nu_8(E_{1u})$ modes may have the nature of the Ni–Cl stretching vibration considering the potential energy distribution.

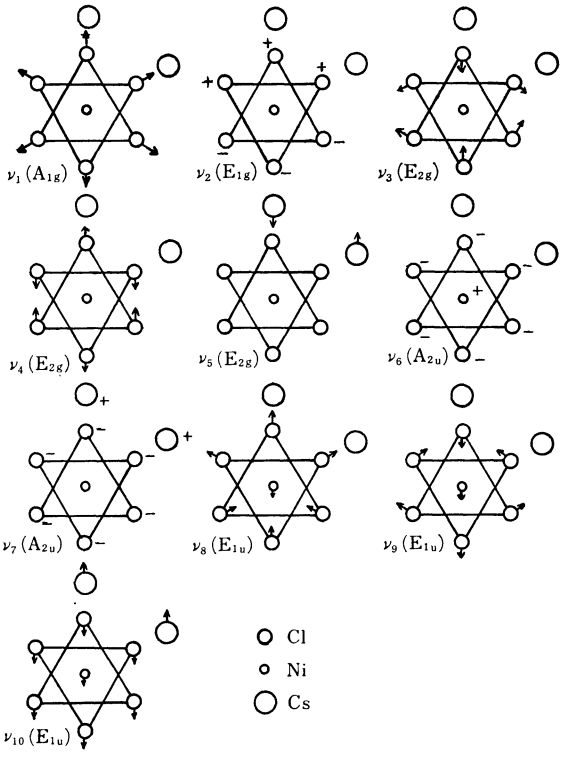

Fig. 6. Displacement of ions for infrared and Raman active vibrations of $CsNiCl_3$ crystal. Projection on the (001) plane.

The authors wish to express their thanks to Professor Mitsuo Ito of Tohoku University for permitting us to use the Raman spectrometer in his laboratory.

References

1) G. L. McPherson and Jin Rong Chang, *Inorg. Chem.*, **12**, 1196 (1973).
2) D. M. Adams and R. R. Smardzewski, *Inorg. Chem.*, **10**, 1127 (1971).
3) G. N. Tischenko, *Jr. Inst. Kristallogr. Akad. Nauk. SSSR.*, **11**, 93 (1955).
4) D. M. Roesller, *Brit. J. Appl. Phys.*, **16**, 1119 (1965). *ibid.*, **17**, 1313 (1966).
5) I. Nakagawa, *Bull. Chem. Soc. Jpn.*, **44**, 3014 (1971).
6) "Far-Infrared Properties of solids," ed by S. S. Mitra and S. Nudelman, Plenum Press New York, London (1970), p. 262.
7) M. Ishii, J. Hiraishi, and H. Takahashi, *Kagaku No Ryoiki*, **27**, 1005 (1973).
8) T. C. Damen, S. P. S. Porto, and B. Tell, *Phys. Rev.*, **142**, 570 (1966).
9) T. Shimanouchi, M. Tsuboi, and T. Miyazawa, *J. Chem. Phys.*, **35**, 1597 (1961).
10) J. Hiraishi, *Bull. Chem. Soc. Jpn.*, **46**, 1334 (1973).
11) E. W. Kellermann, *Phil. Trans. Roy. Soc.*, **238**, 513 (1940).
12) T. Shimanouchi, I. Nakagawa, J. Hiraishi, and M. Ishii, *J. Mol. Spectrosc.*, **19**, 78 (1966).
13) Y. Morioka and I. Nakagawa, *Spectrochim. Acta*, to be published.
14) K. Kohn and I. Nakagawa, *Bull. Chem. Soc. Jpn.*, **43**, 3780 (1970)
15) R. L. Dekock, *Inorg. Chem.*, **10**, 1205 (1971).
16) I. Nakagawa, *Spectrochim. Acta, Part A*, **29**, 1451 (1973).